International Journal of Pharmaceutics 377 (2009) 207–214

Contents lists available at ScienceDirect

International Journal of Pharmaceutics

journal homepage: www.elsevier.com/locate/ijpharm

Pharmaceutical Nanotechnology

Q_{10}-loaded NLC versus nanoemulsions: Stability, rheology and *in vitro* skin permeation

Varaporn B. Junyaprasert[a,*], Veerawat Teeranachaideekul[a,b], Eliana B. Souto[c], Prapaporn Boonme[d], Rainer H. Müller[b]

[a] *Department of Pharmacy, Faculty of Pharmacy, Mahidol University, Thailand*
[b] *Department of Pharmaceutics, Biopharmaceutics and Quality Management, Free University of Berlin, Germany*
[c] *Department of Pharmaceutical Technology, Faculty of Health Sciences, Fernando Pessoa University, Portugal*
[d] *Department of Pharmaceutical Technology, Faculty of Pharmaceutical Sciences, Prince of Songkla University, Thailand*

ARTICLE INFO

Article history:
Received 7 December 2008
Received in revised form 7 May 2009
Accepted 9 May 2009
Available online 22 May 2009

Keywords:
Nanostructured lipid carriers
NLC
Q_{10}
Chemical stability
In vitro skin permeation

ABSTRACT

In this study, nanoemulsions (NE) of medium chain triacylglycerols (MCT) and nanostructured lipid carriers (NLC) of cetyl palmiate/MCT were produced to load coenzyme Q_{10} (Q_{10}) and characterized for their stability before and after incorporation into xanthan gum hydrogels. After storage at 4, 25 and 40 °C, the particles remained in the nanosize range for 12 months, with zeta potential higher than |40 mV|. Similar results were found in xanthan gum-based hydrogels containing NE or NLC. The crystallinity index of Q_{10}-loaded NLC increased after being incorporated into hydrogels. The Q_{10} entrapped in NLC and NE remained higher than 90% at all temperatures for 12 months but dramatically decreased when exposed to light. From the rheological studies, both NLC and NE dispersions possessed pseudoplastic flow having more liquid characteristics, whereas NLC and NE hydrogels exhibited plastic flow with thixothopy, showing more elastic rather than viscous properties. The occurrence of a spatial arrangement of lipid molecules was observed in the matrix of NLC when entrapped into hydrogels. From *in vitro* permeation studies, it could be stated that the amount of Q_{10} released and occlusiveness were major keys to promote the deep penetration of Q_{10} into the skin.

1. Introduction

Skin drug delivery systems have been widely used nowadays for several purposes, e.g. to provide surface effects (e.g., sunscreens, cosmetics, and anti-infectives), dermal effects (e.g., corticosteroids), and systemic effects (e.g., nicotine patches) as well as deeper tissues (e.g. nonsteroidal anti-inflammatory drugs) (Williams, 2003). However, several problems have been reported when the drug is applied via topical/dermal route by the conventional formulations, for instance, low uptake rates due to the barrier functions of stratum corneum and absorption to systemic circulation leading to unwanted systemic side effects (Williams, 2003; Choi and Maibach, 2005). This can be avoided by the use of special approaches that are able to enhance the drug absorption and delivery to the target site. Those are the colloidal drug delivery systems such as liposomes, niosomes, nanoemulsions (NE), solid lipid nanoparticles (SLN) and nanostructured lipid carriers (NLC) (Choi and Maibach, 2005; Müller et al., 2002). SLN and NLC have been introduced as alternative colloidal carrier systems to traditional carriers (e.g. NE, liposomes and polymeric nanoparticles), for both pharmaceutical and cosmetic applications (Müller et al., 2002, 2000). In several publications, many research groups have focused on the application of SLN/NLC for topical/dermal routes (Müller et al., 2002; Wissing et al., 2001; Wissing and Müller, 2001, 2003a; Kalariya et al., 2005; Schüfer-Korting et al., 2007; Üner et al., 2005a). Advantages of SLN/NLC for such purposes include skin occlusion (Wissing and Müller, 2003b; Wissing and Müller, 2002), modulation of drug/cosmetic release (Teeranachaideekul et al., 2007; Souto et al., 2004; Jenning et al., 2000), increase of skin hydration and elasticity (Wissing and Müller, 2003b; Üner et al., 2005a), UV blocking effects (Wissing and Müller, 2001), drug targeting (Schüfer-Korting et al., 2007; Chen et al., 2006; Liu et al., 2007), and enhancement of stability of chemically labile drug/actives (Üner et al., 2005b; Dingler, 1998; Dingler et al., 1999; Jenning and Gohla, 2001; Souto and Müller, 2005). In our previous study, Q_{10}-loaded NLC prepared from different ratios of cetyl palmiate/medium chain triglycerides (oil, MCT), i.e. 95:5, 90:10 and 85:15 were successfully produced by high pressure homogenization (HPH) technique and their physicochemical properties and *in vitro* drug release were compared to the NE solely composed of oil (Teeranachaideekul et al., 2007). The obtained results demonstrated that increasing oil content did not show impact on the mean particle size of NLC but

* Corresponding author. Tel.: +66 26448677x5730; fax: +66 26448694.
E-mail address: pyvbp@mahidol.ac.th (V.B. Junyaprasert).

0378-5173/$ – see front matter © 2009 Elsevier B.V. All rights reserved.
doi:10.1016/j.ijpharm.2009.05.020

rather on the inner structure of NLC and release profiles. Similar finding was reported by Hu et al. (2005, 2006). The higher oil loading led to less order structure of lipid matrix and faster release at the initial stage (Hu et al., 2006, 2005; Teeranachaideekul et al., 2007). However, the data obtained from *in vitro* drug release might not be a relevant method to evaluate the performance of SLN and NLC due to the special feature of occlusiveness described for these particles (Teeranachaideekul et al., 2008). It should be kept in mind that occlusive effect promotes the drug penetration into skin owing to the reducing corneocyte packing and subsequently leading to increasing the inter-corneocytes gaps (Schüfer-Korting et al., 2007). Consequently, enhancement of drug penetration could be facilitated. However, the influence of oil content on the long-term physical and chemical stability of drug entrapped in NLC, as well as on *in vitro* skin permeation using human skin as a membrane have not been elucidated yet. Therefore, the aim of this study was to investigate the effect of increasing the oil loading on the long-term physical and chemical stability of NLC based on cetyl palmitate and MTC. Particle size, zeta potential and degree of crystallinity, as well as viscoelastic properties of aqueous NLC and NE dispersions, were evaluated during storage for 12 months at different temperatures (4, 25 and 40 °C). These properties were monitored after entrapping the carriers into hydrogels, stored for 6 months at 25 °C. The long-term chemical stability of Q_{10}-loaded NLC and NE stored at 4, 25 and 40 °C was monitored for 12 months whereas accelerate stability of Q_{10}-loaded NLC and NE was performed by day light exposure for 28 days. *In vitro* skin permeation studies of Q_{10}-loaded NLC assessed by Franz diffusion cells were evaluated in comparison to Q_{10}-loaded NE.

2. Materials and methods

2.1. Materials

Precifac® ATO (cetyl palmitate), Labrasol® (PEG-8 caprylic/capric triacylglycerols) and Miglyol® 812 (caprylic/capric triacylglycerols) were purchased from Gattefossé (Cedex, France). Tego® Care 450 (Polyglyceryl-3 methylglucose distearate) was obtained from Goldschmidt (Essen, Germany). Q_{10} and xanthan gum were provided by Sigma–Aldrich (Deisenhofen, Germany). Methanol and tetrahydrofuran were obtained from Merck (Darmstadt, Germany). Ultrapurified water was obtained from a MilliQ Plus system, Millipore (Schwalbach, Germany).

2.2. Preparation of NLC and NE

The HPH technique was applied to produce NLC dispersions according to Müller et al. (2000). Briefly, Q_{10} was dissolved in the mixtures of solid and liquid lipids melted approximately 10 °C above the melting point of lipid. Then, the lipid phase was dispersed and admixed to a hot aqueous surfactant solution (80 °C) using an Ultra-Turrax T25 (Janhke & Kunkel GmbH and Co KG, Staufen, Germany) stirred at 8000 rpm for 1 min. Afterwards, the obtained pre-emulsion was homogenized at 80 °C by a high pressure homogenizer for three cycles at 500 bar using an APV Micron Lab 40 (APV system, Unna, Germany). The hot o/w nanoemulsion was cooled to room temperature leading to the lipid phase recrystallization and finally the NLC were formed. In the case of NE, it was produced in the same manner; nonetheless, the solid lipid (cetyl palmitate) was replaced by MCT. The composition of the developed formulations is shown in Table 1. For the formulation of Q_{10}-loaded NLC or NE containing hydrogels, firstly, 2% xanthan gum gel was prepared by dispersing the 2 g of xanthan gum powder in 2.5 ml of propylene glycol, 1% Germaben® and 5 ml of glycerin and subsequently sterile water was added to adjust the final weight. Then 2% xanthan gum gel was formed. To prepare NLC or NE gels, aqueous NLC or NE dispersions were admixed with 2% xanthan gum gel using Ultra-Turrax T25 at the ratio of 10:90 (w/w) (dispersion gel).

2.3. Particle size analysis

Analysis of the particle size was performed by PCS with a Malvern Zetasizer IV (Malvern Instruments, UK). PCS yields the mean particle size (*z*-ave) and the polydispersity index (PI) which is a measure of the width of the size distribution. The *z*-ave and PI values were obtained by averaging of 10 measurements at an angle of 90° in 10 mm diameter cells at 25 °C. Prior to the measurement, all samples were diluted with bidistilled water to have a suitable scattering intensity. The real refractive index and the imaginary refractive index were set at 1.456 and 0.01, respectively. The particle size analysis was determined using the Mie theory. To detect the possible presence of microparticles, the laser diffractometry (LD) (Coulter®LS 230, Beckmann-Coulter Electronics, Krefeld, Germany) with polarization intensity differential scattering (PIDS) was applied. The LD data obtained were evaluated using volume distribution as diameter (*d*) values of 50%, 90% and 99%. The diameter values indicate the percentage of particles possessing a diameter equal or lower than the given value.

2.4. Zeta potential analysis

Zeta potential (ZP) was measured by determining the electrophoretic mobility using Malvern Zetasizer IV. The measurements were performed in distilled water adjusted conductivity to 50 mS/cm with sodium chloride solution (0.9%, w/v). The ZP was calculated using the Helmholtz–Smoluchowsky equation. The measurements were repeated five times at 25 °C with field strength of 20 V/cm. The pH was in the range of 5.5–6.0.

2.5. Differential scanning calorimetry (DSC)

Thermal analysis was performed using a Mettler DSC 821e apparatus (Mettler Toledo, Gieben, Switzerland). The samples were weighed in 40 ml aluminum pans for approximately 1–2 mg based on the lipid content. Heating curves were performed from 25 °C to 85 °C and cooled down to 25 °C at the heating rate of 5 K/min. An empty aluminum pan was used as a reference. The DSC parameters including onset, melting point and enthalpy were evaluated using STARe Software (Mettler Toledo, Switzerland). The crystallinity

Table 1
Compositions of the developed NLC and NE formulations % (w/w).

Formulations	Cetyl palmitate	Miglyol® 812	Tego® Care 450	Q_{10}	Water q.s.
Q_{10}-loaded NE1	–	7.60	1.8	2.4	100
Q_{10}-loaded NLC 1	7.23	0.38	1.8	2.4	100
Q_{10}-loaded NLC 2	6.84	0.76	1.8	2.4	100
Q_{10}-loaded NLC 3	6.46	1.14	1.8	2.4	100
Q_{10}-loaded NLC 4	14.45	0.75	1.8	4.8	100

index (CI) was computed using Eq. (1) (Souto and Müller, 2005; Freitas and Müller, 1999).

$$\mathrm{CI}\,(\%) = \left(\frac{\Delta H_{\mathrm{NLC\ aqueous\ dispersion}}}{\Delta H_{\mathrm{bulk\ material}} \times \mathrm{Concentration}_{\mathrm{lipid\ phase}}} \right) \times 100 \qquad (1)$$

where ΔH_{NLC} and $\Delta H_{\mathrm{bulk\ material}}$ are the melting enthalpy (J/g) of NLC dispersion and bulk lipid, respectively.

2.6. Viscoelastic behavior

The viscoelastic analysis of NLC and NE and gels was performed using a rheometer Rheo Stress RS 100 (Haake Instrument, Karlsruhe, Germany) equipped with a cone-and-plate test geometry (plate diameter 20 mm, cone angle 4°). All measurements were performed at the temperature of 20.0 ± 0.1 °C. Oscillation stress sweep tests were performed at a constant frequency of 1 Hz with a stress between 0 Pa and 100 Pa. Oscillation frequency tests were run over a frequency range of 0.1–10 Hz at a constant stress amplitude under the viscoelastic region (1 Pa) which was previously determined by the oscillation stress sweep tests.

2.7. Long-term chemical stability studies

All samples were kept in siliconized glass vials at different temperatures (4, 25 and 40 °C). The percentage of Q_{10} remaining in NLC and NE formulations was quantified by HPLC at the predetermined time intervals. Briefly, HPLC analysis was performed using a Shimadzu (Kyoto, Japan) running in the isocratic modus. The system consisted of a Shimadzu pump, a Sil-10A Shimadzu auto-injector HPLC and a UV detector. The system consisted of a μBondapack® C18 RP column (Water, Ireland). The mobile phase consisted of 95 parts of methanol and 5 parts of tetrahydrofuran. The injection volume was 20 μl, the flow rate 1 ml/min. The running time was 10 min. All samples were preformed in triplicate. For sample preparation, approximately 100 mg of sample was weighed and dissolved in 10 ml of acetone. Then, it was sonicated in an ultrasonic bath at 20 °C for 10 min for dissolving Q_{10} and lipids. Afterwards, the solution was cooled down to room temperature and it was further injected to the HPLC column.

2.8. In vitro skin permeation studies

2.8.1. Skin preparation

The skin permeation study was carried out with the approval of the Committee on Human Rights Related to Human Experimentation, Mahidol University, Bangkok, Thailand. Human skin samples obtained by abdominoplasty surgeries from female ranging in age from 25 to 60 years were kindly provided by Yahee Hospital, Bangkok, Thailand. The excess adipose layer was sectioned off from the received tissues by dissecting with the surgical scissors. Then, the skin composed of epidermis and underlying dermis was further used for the *in vitro* skin distribution study. For the *in vitro* permeation study, the epidermis was separated from the underlying dermis using the heat separation technique. Briefly, the skin was immersed into a hot water controlled temperature at 60 °C for 1 min. Then, the epidermal layer was carefully separated from the dermis using blunt forceps to produce intact sheets ready for mounting on diffusion cells. The obtained epidermis was wrapped with aluminum foil and stored at −20 °C until used. The stored epidermis was allowed to thaw, cut into 4.5 cm × 4.5 cm pieces and hydrated by placing in isotonic phosphate buffer overnight in a refrigerator (at about 4 °C) before use (Songkro et al., 2003; Junyaprasert et al., 2007).

2.8.2. In vitro permeation study

Prior to *in vitro* permeation studies, skin integrity was evaluated by checking electrical resistance. It has been reported that human epidermal membrane with electrical resistance of higher than 15–20 kΩ cm^2 can be indicative of good integrity (Kasting and Bowman, 1990; Chantasart et al., 2007; Chantasart et al., 2009). Therefore, human epidermal membrane with electrical resistance of higher than 15 kΩ cm^2 was used in this study. *In vitro* permeation studies through human epidermis were investigated using Franz diffusion cells. The diffusion cells were thermo-regulated with a water jacket at 37 °C. The epidermis was excised from human skins and mounted on Franz diffusion cells. The acceptor fluid was collected for 0.5 ml at 8 and 24 h. The amounts of active compound in acceptor fluids and in the epidermis were analyzed by HPLC. At the end of the experiment, the human skins were removed and rinsed with water, isopropanol and subsequently gently dried with a cotton swab. This procedure was done for three times. Then, Q_{10} in human skin was extracted by using the mixtures of chloroform and methanol (2:1, v/v) due to the high solubility of both the Q_{10} and the intercellular lipids of epidermis. Briefly, skins were cut into small pieces and soaked in 3 ml of such mixture for 12 h in a closed tube. Subsequently, the skin pieces were subjected to an ultrasonic for three cycles of 15 min to avoid the raise of the temperature during extraction process. To ensure sufficient extraction of Q_{10} from skin pieces, the residual extracted skin was performed in the same manner as mentioned above. It was found that no HPLC peak signal of Q_{10} was detected in the final extracted solution (LOD = 20 ng/ml) indicating a suitable extraction procedure.

2.9. Statistics

In the present paper, all data were reported as the mean ± standard deviation (SD). Significance of differences was evaluated using Student's *t*-test and one way ANOVA at the probability level of 0.05.

3. Results and discussion

3.1. Particle size analysis by PCS

Fig. 1 shows the mean particle size (*z*-ave) of Q_{10}-loaded NE and NLC evaluated by PCS after production and after storage for 12 months at different temperatures. After production, the *z*-ave of all developed formulations was in the range of 180–250 nm with the PI values of lower than 0.2 indicating a relatively narrow size distribution. Concerning the long-term physical stability of Q_{10}-loaded NLC and NE stored at different temperatures (4, 25 and 40 °C) for 12 months, the *z*-ave of NLC and NE was in the nanosize range and less than 300 nm as well as the PI values of less than 0.3 were obtained at all conditions indicating a good physical stability of these colloidal systems. With respect to the effect of storage temperature on the long-term physical stability of NLC and NE, it was observed that no major difference in the mean particle size of NLC and NE stored at different conditions was detected. From the above results, it could be deduced that both NLC and NE containing Q_{10} were stable at least for 12 months at 4, 25 and 40 °C. Due to the low viscosity of NE and NLC dispersions, it could be assumed that they were not suitable for topical or dermal delivery systems. To cope with this problem, one possibility would be incorporation into hydrogels or creams. In this study, 2% xanthan gum was selected as a gelling agent to increase the viscosity of the dispersions since a low degree of nanoparticle aggregation after incorporation into xanthan gum was reported as compared to other hydorgels (Jenning et al., 2000). Based on the above results, storage temperatures did not affect the mean particle size of Q_{10}-loaded NLC and NE. Thereby, 2% xanthan gum gels

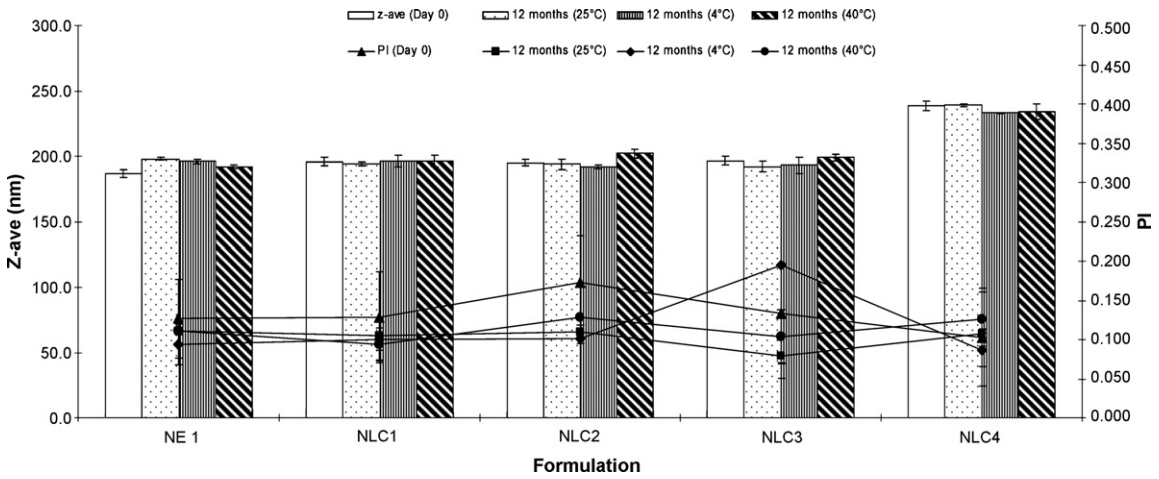

Fig. 1. Mean particle size (*z*-ave) of Q_{10}-loaded NE and NLC dispersions evaluated by PCS after production and after storage for 12 months at 4, 25 and 40 °C.

containing Q_{10}-loaded NLC or NE dispersions were only stored at room temperature (25 °C) so as to evaluate the effect of hydrogels on the mean particle size. The *z*-ave and the PI of Q_{10}-loaded NLC and NE slightly increased after their incorporation into hydrogels in comparison to their original dispersions as seen in Fig. 2. This indicates that the particle aggregation and/or particle growth might occur. After 6 months of storage at room temperature (25 °C), the *z*-ave and the PI of all developed NLC and NE gels were of the same magnitude, i.e. less than 300 nm with a PI of 0.450 (Fig. 2). Conclusively, Q_{10}-loaded NLC and NE after incorporation into hydrogels were stable according to the mean particle size analysis by PCS.

3.2. Particle size analysis by LD

Due to the slow movement and precipitation of large particles, therefore, PCS cannot be applied for detecting the particle size of higher than 6 μm. The large particles can be detected by using LD. The *d*50% determined by LD of 10% Q_{10}-loaded NLC (NLC1, NLC2, and NLC3) and NE (NE1) was less than 150 nm whereas 20% Q_{10}-loaded NLC (NLC4) was less 190 nm after production (data not shown). Comparing the mean particle size by LD (*d*50%) and PCS (*z*-ave), the particle size obtained from LD was smaller than that from PCS. Differences in the mean particle from both methods are due to the fact that PCS measures the intensity fluctuation at hydrodynamic layer of the particle while LD detects the light scattering from the particle surface (Jores et al., 2004). As such, the mean particle size obtained from LD is smaller than that from PCS, particularly when the particle size distribution is narrow. After 12 months of storage at 4, 25 and 40 °C, the *d*50% of all developed NLC and NE dispersions slightly increased, especially for NLC4 (20% lipid phase). The *d*50% of 10% Q_{10}-loaded NLC and NE was less than 165 nm, while that of 20% Q_{10}-loaded NLC (NLC4) was less than 280 nm (data not shown). The presence of considerable amounts of micrometer particles can be excluded for all samples under investigation from the LD results as demonstrated by *d*99% particles which was lower than 450 nm after production. The *d*99% is a good indicative for determining the particle aggregation during storage. After 12 months of storage at different temperatures, the *d*99% of all formulations slightly increased inferring the aggregation of particles. However, the *d*99% was less than 600 nm for all developed formulations as demonstrated in Fig. 3. Concerning the *d*50% of NLC-and NE-based semisolid formulations before and after being incorporated into hydrogels and storage for 6 months at room temperature (25 °C), the *d*50% of all formulations before and after incorporation into hydrogels for 6 months was in the same range (data not shown). This is due to the fact that the samples were stirred during

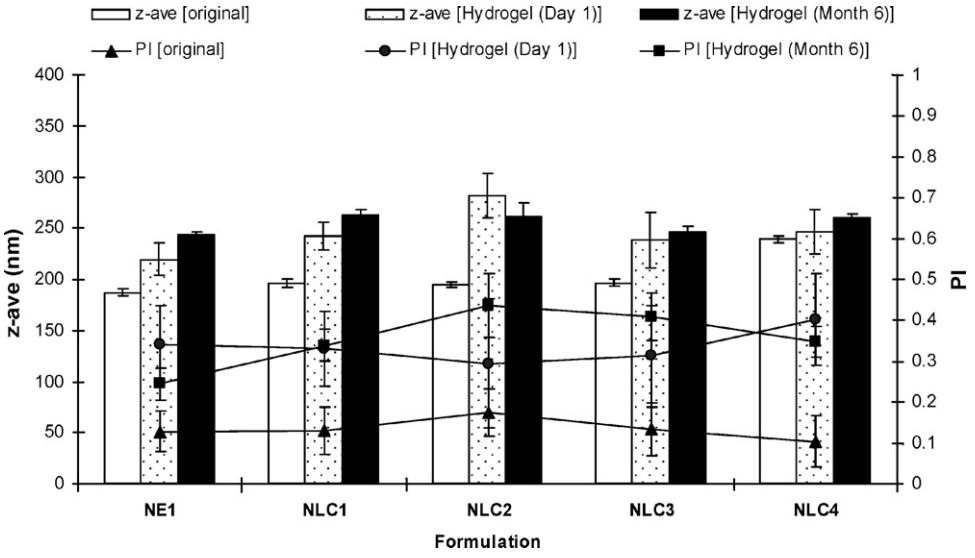

Fig. 2. Mean particle size (*z*-ave) of NLC and NE gels evaluated by PCS after production and during storage for 6 months at 25 °C.

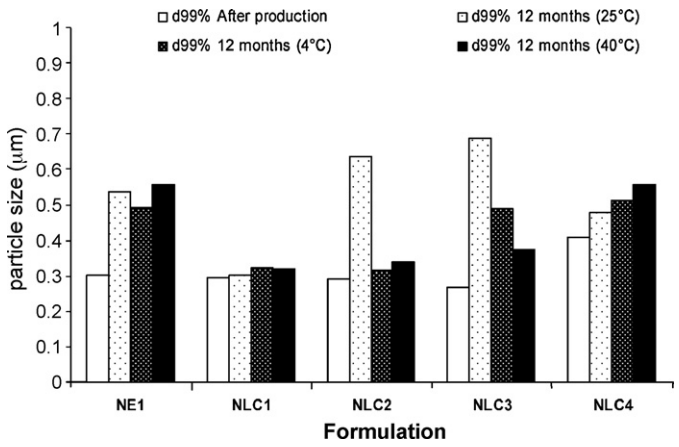

Fig. 3. *d*99% of Q_{10}-loaded NLC and NE dispersions determined by LD after production and after storage for 12 months at 4, 25 and 40 °C.

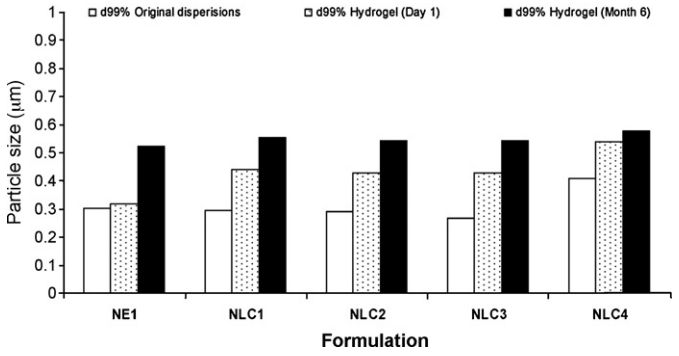

Fig. 4. *d*99% of NLC and NE gels determined by LD after production and after storage for 6 months at 25 °C.

the measurement by LD promoting particle deaggregation. Consequently, the increase in the *z*-ave of NLC-and NE-based semisolid formulations during storage determined by PCS was due to the particle aggregation (particle bridging by hydrogels) rather than the particle growth. Fig. 4 depicts the *d*99% of NLC and NE dispersions before and after incorporation into hydrogels, the incorporation of NLC and NE dispersions into hydrogels increased the *d*99% inferring that the particle aggregation was promoted. However, the *d*99% was less than 600 nm for all developed formulations after incorporation into hydrogels for 6 months at room temperature (25 °C). Thus, it can be concluded that both NLC and NE containing Q_{10} showed a good long-term physical stability before and after being incorporated into hydrogels.

3.3. Zeta potential analysis

In the present study, the ZP values of all developed NLC and NE dispersions after production and storage at different temperature (4, 25 and 40 °C) for 12 months were higher than |−40 mV| indicating a good physical stability of lipid nanoparticles (data not shown). With regard to the ZP values of NLC and NE after incorporation into 2% xanthan gum and storage for 6 months, it was observed that the ZP values of NLC-and NE-based semisolid formulations after production and after storage for 6 months were in the range of |−40 mV| to |−55 mV| similar to the original dispersions (data not shown). From the aforementioned discussion, the ZP values were not affected by the adsorption of hydrogels at the surface of particle leading to the shift of the shear plane and subsequently reduction of ZP values. This might be due to the similar negative charge of particle surface and hydrogels leading to the occurrence of repulsive forces and, as a result, the hydrogels could not be adsorbed on the particle surface.

3.4. DSC investigations

Table 2 shows the DSC parameters, i.e. melting endotherm, onset, enthalpy, and crystallinity index of Q_{10}-loaded NLC after production (day 0) and after storage for 12 months at different temperatures, and of hydrogels containing Q_{10}-loaded NLC after storage at 25 °C for 6 months. After production, the melting point of nanoparticles was lower than that of bulk material (<52 °C) and of the physical mixtures of three components before and after tempering (data not shown). The decrease in the onset and maximum temperature as compared with the bulk material and physical mixtures of three components could be attributed to the effect of the small particle size, which was explained by the Gibbs–Thomson equation. In addition, crystallization can also be affected by the presence of surfactants (Wissing et al., 2004, Zimmermann et al., 2005). During storage for 12 months at 4, 25 and 40 °C, the CI [%] of almost developed NLC dispersions increased but remained below 100%. No gel formation was observed in all

Table 2
DSC parameters of Q_{10}-loaded NLC dispersions obtained after production and storage for 12 months at 4, 25 and 40 °C and of NLC gels determined after incorporation into hydrogels and storage for 6 months at 25 °C.

Formulation	Parameter	After production	12 months (NLC dispersions)			NLC gel (day 1)	NLC gel (month 6)
		25 °C	4 °C	25 °C	40 °C	25 °C	25 °C
NLC1	Melting point (°C)	47.79	47.87	47.83	48.15	48.82	50.06
	Enthalpy (J/g)	14.39	15.70	15.60	16.53	1.70	2.03
	Onset (°C)	45.04	45.06	45.00	44.90	44.87	43.91
	CI [%]	64.58	70.45	70.01	74.18	76.29	91.09
NLC2	Melting point (°C)	47.36	47.47	47.47	47.59	48.12	50.06
	Enthalpy (J/g)	14.29	15.79	15.70	16.34	1.55	1.91
	Onset (°C)	44.76	44.66	44.49	44.36	43.90	43.07
	CI [%]	64.13	70.86	70.45	73.33	69.56	85.71
NLC3	Melting point (°C)	47.32	47.08	47.11	44.73	48.23	49.12
	Enthalpy (J/g)	12.45	14.86	11.94	12.84	1.32	1.56
	Onset (°C)	44.90	44.20	44.64	44.73	44.26	42.62
	CI [%]	55.87	66.68	53.58	57.62	59.24	70.00
NLC4	Melting point (°C)	48.30	48.32	48.32	50.41	49.53	49.57
	Enthalpy (J/g)	31.49	32.80	30.90	38.79	3.49	3.89
	Onset (°C)	45.36	44.96	44.94	48.82	46.28	45.08
	CI [%]	70.66	73.60	69.33	87.04	78.31	87.28

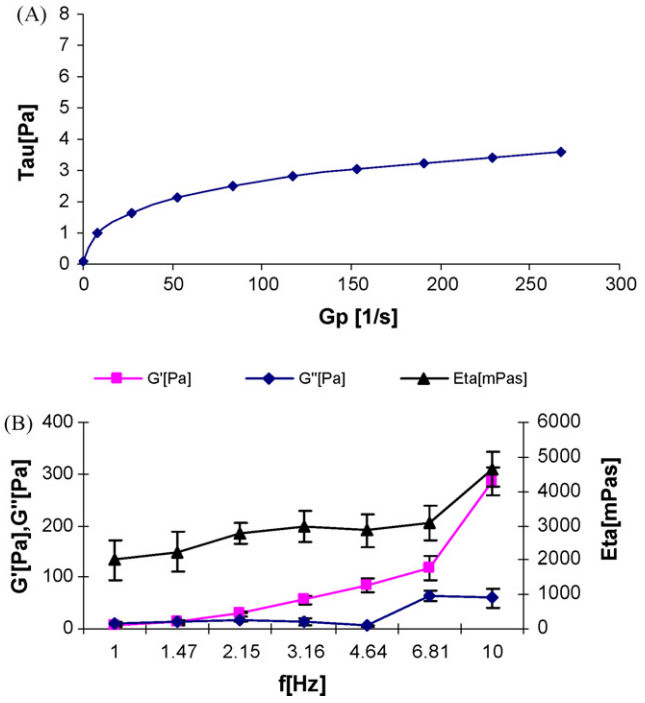

Fig. 5. Rheological measurement of Q_{10}-loaded NLC1 after production: (A) shear stress as a function of shear rate at 20 °C and (B) oscillation frequency sweep test at a stress of 1 Pa at 20 °C.

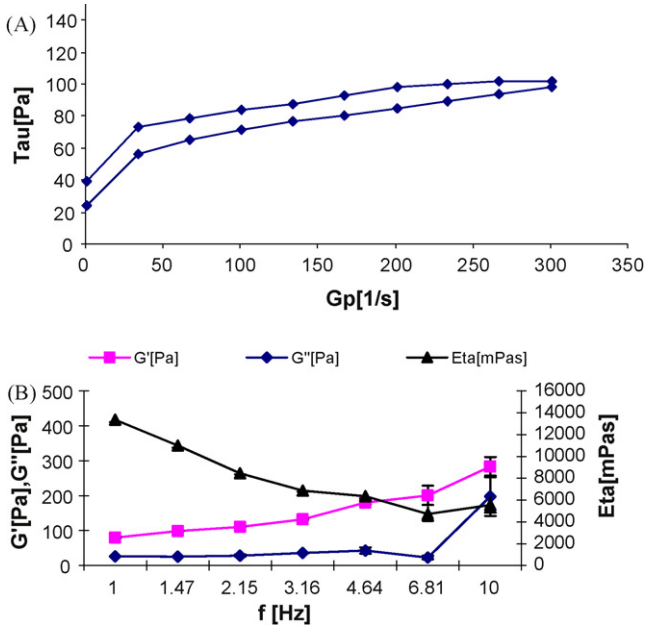

Fig. 6. Rheological measurement of Q_{10}-loaded NLC gels after production: (A) shear stress as a function of shear rate at 20 °C and (B) oscillation frequency sweep test at a stress of 1 Pa at 20 °C.

developed formulations. Concerning the CI [%] values of hydrogels containing Q_{10}-loaded NLC, incorporation of particles in the developed hydrogels noticeably accelerated the lipid recrystallization as indicated by an increase in the CI [%]. Similar findings have also been reported for ascorbyl palmitate-loaded SLN or NLC after incorporation into Carbopol-based hydrogels (Üner et al., 2004). This behavior indicates that hydrogels can accelerate the organization of inner structure of NLC. In a previous report, polymorphic transitions can be accelerated by the presence of a drug in the carrier (Schwarz and Mehnert, 1999). In the present work, it has been shown that the inner structure of NLC is also influenced by the viscosity enhancer, i.e. xanthan gum, which might further lead to the drug expulsion from lipid nanoparticles. By means of polarized optical microscopy, however, no Q_{10} crystals were detected in xanthan gum-based hydrogels containing Q_{10}-loaded NLC and NE after 6 months of storage at room temperature (data not shown).

3.5. Rheological analysis of Q10-loaded NLC and NE dispersions

From continuous shear rheometry, Q_{10}-loaded NLC and NE dispersions revealed pseudoplastic flow where the shear rate increased with the increasing shear stress with a yield value of practically zero (Fig. 5A). Moreover, a weak structure had been characterized after applying an oscillation test, revealing high liquid properties indicated a higher loss modulus (G'') in comparison to the storage modulus (G') at the low frequency (Fig. 5B). After being incorporated into hydrogles, NLC and NE gels showed a plastic flow. The shear rate increased with the increasing shear stress followed by a thixotropic behavior where ascending and descending flow curves did not overlap (Fig. 6A).

Concerning the G' and G'' of the NLC and NE gels within the linear viscoelastic region (1 Pa), all developed formulations showed the G' values much higher than the G'' values, indicating a more elastic rather than viscous behavior. Besides, the η^* depended on the frequency, i.e. decreased with the increasing frequency which is typical for plastic materials (Fig. 6B). Fig. 7 depicts the G' values of NLC and NE gels during storage time of 6 months. It can be seen that G' measured at a frequency of 1 Hz of all NLC gel formulations slightly increased. The change in the G' was not caused by a change in the mean particle size (Fig. 2) but rather by the spatial arrangement of the lipid molecules in NLC matrix. This is related to the increasing CI [%] of NLC gels during storage. Furthermore, this event was not observed for NE gels. As mentioned above, the increase in CI [%] of Q_{10}-loaded NLC dispersions was accelerated after incorporation into hydrogels. According to the applied oscillation test, it has been detected an increase in G' of hydrogel containing Q_{10}-loaded NLC during storage time at the applied frequency of 1 Pa. This was not observed for hydrogels containing Q_{10}-loaded NE dispersions as well as for Q_{10}-loaded NLC and NE dispersions during storage (data not shown). Again, these results point out the occurrence of spatial arrangements within NLC matrix during storage time, particularly after their incorporation into hydrogels.

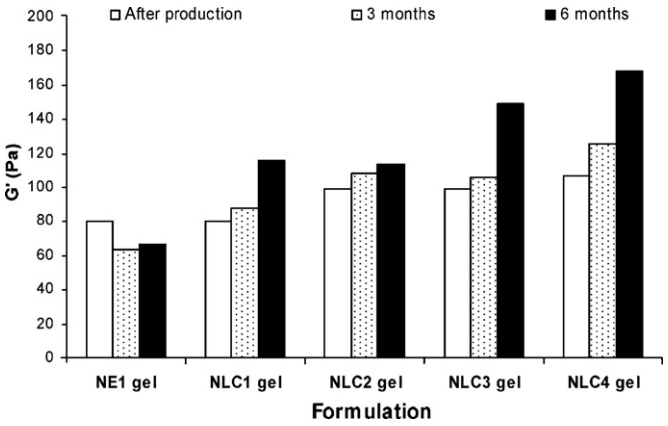

Fig. 7. Storage modulus (G') of NLC and NE gels recorded after production, 3 months and 6 months at a frequency of 1 Hz at 20 °C.

Table 3
Percent Q_{10} remaining after 12 months of storage at 4, 25 and 40 °C and after exposure to the day light for 14 and 28 days.

Formulation	% Q_{10} remaining after 12 months			% Q_{10} remaining after exposure to day light	
	4 °C	25 °C	40 °C	14 days	28 days
NE1	96.87 ± 0.45	98.82 ± 0.35	91.49 ± 1.14	77.35 ± 0.54	46.00 ± 0.41
NLC1	101.17 ± 0.38	100.30 ± 1.50	96.86 ± 0.98	83.02 ± 0.94	51.94 ± 0.52
NLC2	99.26 ± 0.59	100.66 ± 4.31	95.80 ± 2.71	86.74 ± 0.50	51.03 ± 0.35
NLC3	96.81 ± 0.47	97.60 ± 1.71	92.20 ± 0.07	84.37 ± 1.07	48.22 ± 0.34
NLC4	97.51 ± 0.61	101.02 ± 0.22	93.54 ± 0.62	90.03 ± 1.55	75.04 ± 0.71

3.6. Long-term chemical stability of Q_{10}-loaded NLC and NE dispersions

With regard to Q_{10} entrapped in NLC and NE, a good chemical stability of all formulations was observed, i.e. the percentage of active remaining within the systems was higher than 90% when stored at 4, 25 and 40 °C for 12 months. Nevertheless, these results were highly influenced by the storage temperature (Table 3). The chemical stability of Q_{10} in all formulation stored at 40 °C was lower than at 4 and 25 °C. Comparing the effect of oil content in the NLC, the chemical stability of Q_{10} stored at 40 °C tended to decrease when increasing the oil content, which can be attributed to the accumulation of Q_{10} at the surface of lipid nanoparticles. This observation was confirmed with the previous study of *in vitro* release studies using Franz diffusion cells (Teeranachaideekul et al., 2007). In order to challenge the system, the chemical stability of Q_{10} was investigated under stress conditions, e.g., exposure to the day light. The accelerated chemical stability of Q_{10} entrapped NLC and NE was assessed by exposing the formulations to day light at 25 °C (Table 3). The results demonstrated that the chemical stability of Q_{10} in both NLC and NE dramatically decreased, especially for NE. The percentage of Q_{10} remaining after exposure to day light for 28 days formulated in NLC was higher than that of NE ($p < 0.05$). Comparing the results among NLC formulations, the percentage of Q_{10} depended on the oil content in the formulation. The obtained data from accelerated chemical stability test by exposing the formulations to day light are in agreement with those from long-term chemical stability analysis. During storage under day light exposure, the viscosity of all NLC dispersions increased as observed visually and finally gel formation occurred. In a previous study, gel formation was reported by exposure of SLN to the light, being also dependent on the light intensity, e.g., the higher the intensity, the higher the velocity (Freitas and Müller, 1999). From the above results, it can be concluded that the enhancement of chemical stability of Q_{10} can be achieved when it is formulated preferentially in NLC than in NE.

3.7. In vitro permeation study

Q_{10} penetration into excised human skin (epidermis) treated with Q_{10}-loaded NLC and NE was analyzed after 8 and 24 h. The amount of Q_{10} was quantified in skin and in a suitable acceptor medium. Due to lipophilic characteristic of Q_{10}, phosphate buffer pH 7.4 and Labrasol® in the ratio of 95 and 5 (w/w) was used as the acceptor medium in order to achieve sink conditions. Fig. 8 shows the amount of Q_{10} in the epidermis and in the acceptor medium after applying the formulations for 8 and 24 h. The amount of Q_{10} in the epidermis and in the acceptor medium relied on the colloidal type for 10% lipid dispersion (NE1, NLC1, NLC2 and NLC3). No significant differences were observed in the total amounts of Q_{10} (Q_{10} in the epidermis plus in the acceptor medium) after applying the formulations for 8 h ($p > 0.05$) (Fig. 8). However, from the *in vitro* drug release studies as reported in our previous study, the cumulative amount of Q_{10} released from Q_{10}-loaded NLC1 was lower than that of Q_{10}-loaded NLC2, NLC3 and of Q_{10}-loaded NE1 (Teeranachaideekul et al., 2007). This means that not only the high amount of Q_{10} released from carriers but also occlusiveness can be pointed out as the major keys to promote and subsequently enhance the drug penetration into the deep skin (acceptor medium). Q_{10}-loaded NLC3 provided the higher amount of Q_{10} in the acceptor medium than Q_{10}-loaded NE1 (Fig. 8A). This was due to the higher Q_{10} released from Q_{10}-loaded NLC3, as well as to the film formation of NLC enhancing the Q_{10} penetration into the acceptor medium. After 24 h, the highest total amount of Q_{10} was found when applying Q_{10}-loaded NE1 (Fig. 8B). This is due to the fact that the high amount of Q_{10} was released from NE in comparison to NLC whereas Q_{10}-loaded NLC revealed sustained release patterns. Therefore, the high amount of Q_{10} released from NE promoted the penetration of Q10 into the skin. Nonetheless, the amount of Q_{10} in the acceptor medium was not significantly different after applying NE and NLC for 24 h due to the lower occlusiveness of NE as compared to NLC. Since Q_{10} has been quantified in the acceptor medium, occlusive effect could therefore enhance the penetration of drug into deep skin. Concerning the *in vitro* skin permeation study of Q_{10}-loaded NLC, after 8 h the total amount of Q_{10} was not significantly different after applying Q_{10}-loaded NLC1, NLC2 and NLC3 ($p > 0.05$). During the *in vitro* skin permeation studies, film formation was observed after applying NLC dispersions onto the human skin. The film formation was completely visualized for 2, 3, and 5 h after applying Q_{10}-loaded NLC1, NLC2 and NLC3, respectively. This film formation could promote the penetration of Q_{10} released from NLC into the

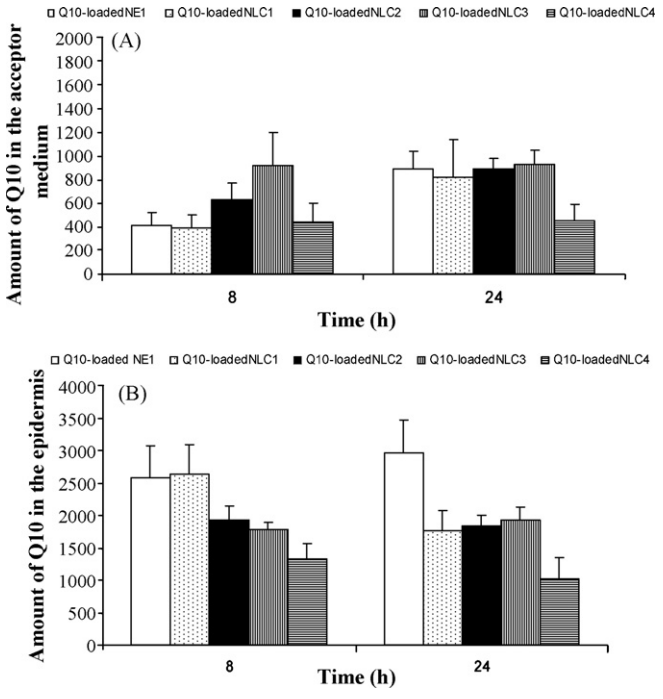

Fig. 8. *In vitro* skin permeation study of Q_{10}-loaded NLC and NE dispersions after applying for 8 and 24 h (A): amount of Q_{10} in an acceptor medium and (B): amount of Q_{10} into skin ($n = 6–8$).

skin, particularly from Q_{10}-loaded NLC1. This might be the reason why the total amount of Q_{10} (Q_{10} in the epidermis plus the acceptor medium) from Q_{10}-loaded NLC1, which showed the lowest Q_{10} released according to *in vitro* drug release (Teeranachaideekul et al., 2007), was similar to that from Q_{10}-loaded NLC2 and NLC3. The amount of Q_{10} in the acceptor medium after applying Q_{10}-loaded NLC3 on the skin for 8 h was higher than that from Q_{10}-loaded NLC2 and NLC1, respectively. This was attributed to the high amount of Q_{10} released from the Q_{10}-loaded NLC3, together with the occlusiveness leading to the deeper penetration of Q_{10} detected in the acceptor medium. Comparing the *in vitro* permeation of Q_{10}-loaded NLC1 and NLC4, it was found that the former one showed the higher total amount of Q_{10} (Q_{10} in the epidermis plus in the acceptor medium) after applying for 8 and 24 h (Fig. 8). This is due to the difference in the encapsulation models, i.e. drug-enriched core for Q_{10}-loaded NLC4 and drug-enriched shell for Q_{10}-loaded NLC1 leading to the difference in Q_{10} penetration (Teeranachaideekul et al., 2007). Moreover, the mean particle size of Q_{10}-loaded NLC4 (~230 nm) was larger than that of Q_{10}-loaded NLC1 (~190 nm) ($p < 0.05$) resulting in a lower occlusive effect.

4. Conclusion

The Q_{10}-loaded NLC dispersions composed of varying solid lipid/oil ratios demonstrated good long-term physical and chemical stability as indicated by the particle size determined by PCS and LD, the zeta potential value and the percentage of Q_{10} remaining in the formulation. From the accelerate chemical stability results, the chemical stability of Q_{10} entrapped in NLC was higher than that in NE and relied on the amount of oil content in NLC, i.e. the higher oil content, the lower percent Q_{10} remaining. The increase in CI [%] and storage modulus (G') during storage time of Q_{10}-loaded NLC dispersions was accelerated when incorporation into hydrogels demonstrating that the crystallization process and the spatial arrangement of NLC dispersions could be induced by incorporation of NLC into hydrogel. With respect to the *in vitro* permeation study, the amount of Q_{10} in the skin and acceptor medium was affected by the amount of oil content in NLC and the occlusive effect.

Acknowledgements

Financial support from the Thailand Research Fund (TRF) through the Royal Golden Jubilee Ph.D. Program (Grant No. PHD/0160/2546) and the TRF-Master Research Grants (MRGOS-MEP505S176) and from the German Academic Exchange Service (DAAD) is gratefully acknowledged.

References

Chantasart, D., Pongjanyakul, T., Higuchi, W.I., Li, S.K., 2009. Effects of oxygen-containing terpenes as skin permeation enhancers on the lipoidal pathways of human epidermal membrane. J. Pharm. Sci., doi:10.1002/jps.21666.

Chantasart, D., Sa-Nguandeekul, P., Prakongpan, S., Li, S.K., Higuchi, W.I., 2007. Comparison of the effects of chemical permeation enhancers on the lipoidal pathways of human epidermal membrane and hairless mouse skin and the mechanism of enhancer action. J. Pharm. Sci. 96, 2310–2326.

Chen, H., Chang, X., Du, D., Liu, W., Liu, J., Weng, T., Yang, Y., Xu, H., Yang, X., 2006. Podophyllotoxin-loaded solid lipid nanoparticles for epidermal targeting. J. Control. Release 110, 296–306.

Choi, M.J., Maibach, H.I., 2005. Liposomes and niosomes as topical drug delivery systems. Skin. Pharmacol. Physiol. 18, 209–219.

Dingler, A., 1998. Feste lipid-nanopartikel als kolloidale wirkstofftragersysteme zur dermalen applikation. Free University of Berlin, Berlin.

Dingler, A., Blum, R.P., Niehus, H., Mller, R.H., Gohla, S., 1999. Solid lipid nanoparticles (SLN/Lipopearls)—a pharmaceutical and cosmetic carrier for the application of vitamin E in dermal products. J. Microencapsul. 16, 751–767.

Freitas, C., Müller, R.H., 1999. Correlation between long-term stability of solid lipid nanoparticles (SLN) and crystallinity of the lipid phase. Eur. J. Pharm. Biopharm. 47, 125–132.

Hu, F.Q., Jiang, S.P., Du, Y.Z., Yuan, H., Ye, Y.Q., Zeng, S., 2005. Preparation and characterization of stearic acid nanostructured lipid carriers by solvent diffusion method in an aqueous system. Colloids Surf. B: Biointerfaces 45, 167–173.

Hu, F.Q., Jiang, S.P., Du, Y.Z., Yuan, H., Ye, Y.Q., Zeng, S., 2006. Preparation and characteristics of monostearin nanostructured lipid carriers. Int. J. Pharm. 314, 83–89.

Jenning, V., Gohla, S.H., 2001. Encapsulation of retinoids in solid lipid nanoparticles (SLN). J. Microencapsul. 18, 149–158.

Jenning, V., Schäfer-Korting, M., Gohla, S., 2000. Vitamin A-loaded solid lipid nanoparticles for topical use: drug release properties. J. Control. Release 66, 115–126.

Jores, K., Mehnert, W., Drechsler, M., Bunjes, H., Johann, C., Mader, K., 2004. Investigations on the structure of solid lipid nanoparticles (SLN) and oil-loaded solid lipid nanoparticles by photon correlation spectroscopy, field-flow fractionation and transmission electron microscopy. J. Control. Release 95, 217–227.

Junyaprasert, V.B., Boonme, P., Songkro, S., Krauel, K., Rades, T., 2007. Transdermal delivery of hydrophobic and hydrophilic local anesthetics from o/w and w/o brij 97 based microemulsions. J. Pharm. Pharm. Sci. 10, 288–298.

Kalariya, M., Padhi, B.K., Chougule, M., Misra, A., 2005. Clobetasol propionate solid lipid nanoparticles cream for effective treatment of eczema: Formulation and clinical implications. Indian J. Exp. Biol. 43, 233–240.

Kasting, G.B., Bowman, L.A., 1990. DC electrical properties of frozen, excised human skin. Pharm. Res. 7, 134–143.

Liu, J., Hu, W., Chen, H., Ni, Q., Xu, H., Yang, X., 2007. Isotretinoin-loaded solid lipid nanoparticles with skin targeting for topical delivery. Int. J. Pharm. 328, 191–195.

Müller, R.H., Mäder, K., Gohla, S., 2000. Solid lipid nanoparticles (SLN) for controlled drug delivery—a review of the state of the art. Eur. J. Pharm. Biopharm. 50, 161–177.

Müller, R.H., Radtke, M., Wissing, S.A., 2002. Solid lipid nanoparticles (SLN) and nanostructured lipid carriers (NLC) in cosmetic and dermatological preparations. Adv. Drug Deliv. Rev. 54, S131–S155.

Schüfer-Korting, M., Mehnert, W., Korting, H.C., 2007. Lipid nanoparticles for improved topical application of drugs for skin diseases. Adv. Drug Deliv. Rev. 59, 427–443.

Schwarz, C., Mehnert, W., 1999. Solid lipid nanoparticles (SLN) for controlled drug delivery. II. Drug incorporation and physicochemical characterization. J. Microencapsul. 16, 205–213.

Songkro, S., Purwo, Y., Becket, G., Rades, T., 2003. Investigation of newborn pig skin as an *in vitro* animal model for transdermal drug delivery. STP Pharma Sci. 13, 133–139.

Souto, E.B., Müller, R.H., 2005. SLN and NLC for topical delivery of ketoconazole. J. Microencapsul. 22, 501–510.

Souto, E.B., Wissing, S.A., Barbosa, C.M., Müller, R.H., 2004. Development of a controlled release formulation based on SLN and NLC for topical clotrimazole delivery. Int. J. Pharm. 278, 71–77.

Teeranachaideekul, V., Boonme, P., Souto, E.B., Müller, R.H., Junyaprasert, V.B., 2008. Influence of oil content on physicochemical properties and skin distribution of Nile red-loaded NLC. J. Control. Release 128, 134–141.

Teeranachaideekul, V., Souto, E.B., Junyaprasert, V.B., Müller, R.H., 2007. Cetyl palmitate-based NLC for topical delivery of coenzyme Q_{10}—development, physicochemical characterization and in vitro release studies. Eur. J. Pharm. Biopharm. 67, 141–148.

Üner, M., Wissing, S.A., Yener, G., Müller, R.H., 2004. Influence of surfactants on the physical stability of solid lipid nanoparticle (SLN) formulations. Pharmazie 59, 331–332.

Üner, M., Wissing, S.A., Yener, G., Müller, R.H., 2005a. Skin moisturizing effect and skin penetration of ascorbyl palmitate entrapped in solid lipid nanoparticles (SLN) and nanostructured lipid carriers (NLC) incorporated into hydrogel. Pharmazie 60, 751–755.

Üner, M., Wissing, S.A., Yener, G., Müller, R.H., 2005b. Solid lipid nanoparticles (SLN) and nanostructured lipid carriers (NLC) for application of ascorbyl palmitate. Pharmazie 60, 577–582.

Williams, A., 2003. Structure and function of human skin. In: Williams, A. (Ed.), Transdermal and Topical Drug Delivery. Pharmaceutical Press, London, pp. 1–26.

Wissing, S., Lippacher, A., Müller, R., 2001. Investigations on the occlusive properties of solid lipid nanoparticles (SLN). J. Cosmet. Sci. 52, 313–324.

Wissing, S.A., Müller, R.H., 2001. Solid lipid nanoparticles (SLN)—a novel carrier for UV blockers. Pharmazie 56, 783–786.

Wissing, S.A., Müller, R.H., 2002. Solid lipid nanoparticles as carrier for sunscreens: *In vitro* release and *in vivo* skin penetration. J. Control. Release 81, 225–233.

Wissing, S.A., Müller, R.H., 2003a. Cosmetic applications for solid lipid nanoparticles (SLN). Int. J. Pharm. 254, 65–68.

Wissing, S.A., Müller, R.H., 2003b. The influence of solid lipid nanoparticles on skin hydration and viscoelasticity—*in vivo* study. Eur. J. Pharm. Biopharm. 56, 67–72.

Wissing, S.A., Müller, R.H., Manthei, L., Mayer, C., 2004. Structural characterization of Q_{10}-loaded solid lipid nanoparticles by NMR spectroscopy. Pharm. Res. 21, 400–405.

Zimmermann, E., Souto, E.B., Müller, R.H., 2005. Physicochemical investigations on the structure of drug-free and drug-loaded solid lipid nanoparticles (SLN) by means of DSC and ^{1}H NMR. Pharmazie 60, 508–513.